Electrochemistry Communications 114 (2020) 106702

Contents lists available at ScienceDirect

Electrochemistry Communications

journal homepage: www.elsevier.com/locate/elecom

Full Communication

On-line monitoring of dissolution processes in nonaqueous electrolytes – A case study with platinum

Johanna Ranninger[a,b,*], Susanne J. Wachs[a,b], Jonas Möller[a], Karl J.J. Mayrhofer[a,b], Balázs B. Berkes[a,*]

[a] Helmholtz Institute Erlangen-Nürnberg for Renewable Energy (IEK-11), Forschungszentrum Jülich GmbH, 91058 Erlangen, Germany
[b] Department of Chemical and Biological Engineering Friedrich-Alexander-Universität Erlangen-Nürnberg, 91058 Erlangen, Germany

ARTICLE INFO

Keywords:
Nonaqueous electrochemistry
Platinum dissolution
Anodic dissolution
Methanol-based electrolyte
Organic ICP-MS
On-line dissolution monitoring

ABSTRACT

Fundamental understanding of electrochemistry in nonaqueous electrolytes is important for applications like nonaqueous batteries, electroorganic synthesis, CO_2 reduction, or metal deposition. Studies on electrode stability contribute to our fundamental understanding and are essential for the evaluation of the overall performance of electrochemical systems. With this work we introduce a tool to this field aiming to particularly investigate dissolution of different electrode materials qualitatively and quantitatively in water-free, organic media. The new approach consists of an electroanalytical flow cell with scanning capability on-line coupled to an inductively coupled plasma mass spectrometer, all together optimized to harsh organic environments. As a case study to demonstrate the strength of the method, we have chosen platinum as working electrode. We unveil its dissolution behavior in methanol-based organic electrolytes for the first time under controlled atmosphere (glovebox), and demonstrate differences in dissolution mechanism compared to aqueous electrolytes.

1. Introduction

Organic electrolytes have several advantages over aqueous ones, which are among others the wider electrochemical and temperature stability window, better solubility of several substances with interesting electrochemistry or tunable physico-chemical properties through the use of mixtures. In the past decades, research in this field has been intensified due to the growing applications of battery technologies like lithium ion, lithium air, or lithium sulfur batteries, as well as striking progress in other areas like sensors, capacitors and organic electrosynthesis [1–4].

Half-cell investigations, like in classical electrochemistry, in air- and water-free, nonaqueous electrolytes are less common, yet essential for establishing a fundamental understanding of reaction mechanisms, activity parameters, or stability and selectivity. Particularly on-line coupled analytics to electrochemical flow cells have proven to be crucial in obtaining complementary, time-resolved information on reaction products and dissolution. Differential electrochemical mass spectrometry has been utilized both in aqueous [5] and organic electrolytes [6] for the analysis of reaction products in diverse reactions. A series of studies on stability have been carried out in aqueous systems with sophisticated in situ methods [7–10]. The coupling of an electrochemical scanning flow cell (SFC) with an inductively coupled plasma mass spectrometer (ICP-MS) has been proven to be a beneficial tool to study dissolution of electrode materials on-line in aqueous systems in a high through-put mode [11,12]. Those studies gave valuable insights into the electrode degradation mechanisms and processes [13–15]. In organic electrolytes, dissolution of metals has only recently been monitored in situ with a coupled electrochemical technique [16–18]. However, so far both the sensitivity of detection as well as the completely O_2-free operation has been a major challenge. In this work we present the development of an electroanalytical flow cell (EFC) – ICP-MS setup for nonaqueous electrolyte systems and demonstrate its capabilities showing Pt dissolution profiles in a methanol-based electrolyte. Although platinum metal and its dissolution are well-studied in electrochemistry [19–21], we demonstrate new aspects of its behavior regarding dissolution mechanisms. With this work we pave the way for a series of studies focusing on understanding the stability of electrode materials in organic electrochemical systems eventually contributing to the development of improved electrode materials and/or operating conditions.

2. Experimental methods

The development of the EFC – ICP-MS setup for nonaqueous

* Corresponding authors.
E-mail addresses: j.ranninger@fz-juelich.de (J. Ranninger), b.berkes@fz-juelich.de (B.B. Berkes).

https://doi.org/10.1016/j.elecom.2020.106702
Received 10 February 2020; Received in revised form 24 February 2020; Accepted 24 February 2020
Available online 06 March 2020

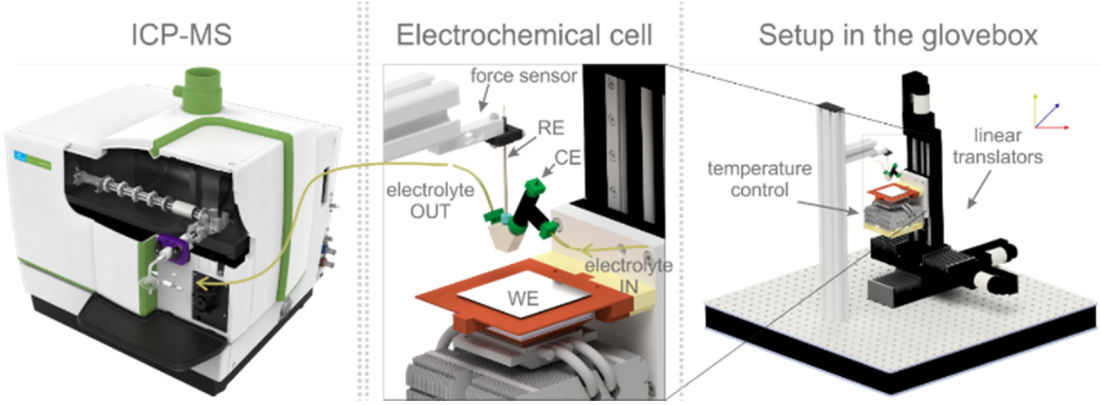

Fig. 1. Schematics of the experimental setup showing the electrochemical flow cell coupled to the ICP-MS.

electrolytes will be discussed in detail in the results section. Fig. 1 shows a representation of the EFC coupled to the ICP-MS. All electrochemical measurements and sample preparations were carried out in an argon filled glovebox (MBRAUN) where the levels of water and oxygen were kept below 1 ppm to prevent contamination of the electrolytes with O_2 and H_2O. Additionally, the water content of the nonaqueous electrolytes was determined using a Karl Fischer 917 Coulometer (Metrohm), also placed in the glovebox. A Biologic VSP 300 potentiostat was used to perform the electrochemical measurements. Polycrystalline platinum foil (99.99% MaTecK) served as the working electrode (WE) and was polished with 0.3 μm Al_2O_3 paste on a MD-Mol polishing cloth (Struers) before each use. The counter electrode (CE), a glassy carbon rod (HTW Hochtemperatur-Werkstoffe GmbH), was rinsed with acetone, isopropyl alcohol, ethanol and ultra-pure water (PURELAB flex, Elga), respectively, prior to use. As reference electrode (RE) a homemade leakage free RE (cell body purchased from Innovative Instruments, Inc.) with a Ag wire immersed in 0.1 mol L^{-1} tetrabutylammonium perchlorate and 0.01 mol L^{-1} $AgNO_3$ in methanol were used. The WE, CE and EFC with fittings and tubing were dried overnight in a VO400 vacuum oven (Memmert GmbH & Co. KG) at 60 °C. The electrolyte was pumped through the EFC with a flow rate of 150 μL min^{-1} using a Legato® 100 syringe pump (KD Scientific). The outlet of the EFC was directly connected to a NexION 2000 ICP-MS (PerkinElmer), whereas the internal standard, 10 μg L^{-1} $(NH_4)ReO_4$ in water (Certipur®, Merck) dissolved in ethanol, was added over a Y-piece with the same flow rate via the built-in peristaltic pump of the ICP-MS (MP2). Ethanol was chosen to introduce the internal standard flow into the analyte flow because of its lower toxicity and excellent miscibility with methanol. Water, on the other hand, was ruled out as internal standard solvent because the miscibility was not sufficient and no stable analyte signals were obtained. For the calibration of the instrument H_2PtCl_6 in HCl 7% (Certipur®, Merck) dissolved in electrolyte matrix was used. The cyclic voltammetry (CV) curves were validated with a classical electrochemical setup, consisting of an undivided glass cell and electrodes of the same kind as for the flow cell experiments, for reproducible results.

All chemicals were used as purchased without further purification. The nonaqueous electrolytes were prepared from $LiClO_4$ (battery grade, dry, 99.99% trace metals basis, Sigma Aldrich) and methanol (max. water content 0.003%, SeccoSolv, Merck). The water content of the prepared solutions measured by Karl-Fischer titration in the glovebox was 37 ppm.

3. Results and discussion

3.1. Considerations for the development of the electrochemical setup for nonaqueous electrolytes

The first step towards the development of an electroanalytical flow cell for nonaqueous systems was choosing the right materials. For tubing, cell body material and connections polytetrafluoroethylene (PTFE) and fluorinated ethylene propylene (FEP), polyether ether ketone (PEEK) and perfluoroalkoxy alkane (PFA) were used. The cell was in-house manufactured in a 60° V-shaped channel design with channel diameters of 1.6 mm [22]. At the bottom of the cell a milled groove was added to fit the homemade FFKM flat seal (Kalrez®) that defined the contact area of the working electrode to be 4.34 mm^2.

One of the main differences comparing nonaqueous with aqueous electrochemistry is the low conductivity. In order to overcome this issue, the electrodes incorporated into the flow cell had to be positioned in close proximity to each other. Therefore, the counter electrode was put in the inlet of the flow cell using a T-piece, which allowed a minimal distance between CE and WE. The RE was positioned opposite of the WE in a distance of 2–3 mm to keep the internal resistance as low as possible (see Fig. 1 for details). For the nonaqueous electrolyte system used in this study the internal resistance was 340 Ω, which was compensated using manual IR compensation (software 85%).

In order to control the force used to press the cell against the WE, the flow cell was attached to a force sensor (ME Meßsysteme GmbH). The cell was positioned on the WE surface using three linear axes (Physik Instrumente (PI) GmbH & Co. KG) moving the WE to the desired position. This setup also allows scanning of the WE surface, which has several advantages to traditional flow cells [12]. All devices except the ICP-MS involved in the measurements were controlled via a homemade LabVIEW software.

In organic electrochemistry typically used electrolytes consist of tetraalkylammonium (TAA), lithium, or sodium cations, but others are also possible depending on the application. The most common anions are perchlorate, hexafluorophosphate or tetrafluoroborate [23]. The total dissolved solids (TDS) of the samples for analysis in the ICP-MS should be kept around 0.2% in order to avoid matrix component deposition on the cones which might lead to instrument instability and signal decrease over the course of a measurement [24,25]. For this study we chose $LiClO_4$ as supporting electrolyte in a concentration of 0.05 mol L^{-1} because of its lower molecular weight compared to TAA salts.

The choice of the right RE is crucial in nonaqueous electrochemistry. Various suggestions have been made, ranging from aqueous REs for short measurements over quasi REs to real nonaqueous REs that are filled with the same electrolyte like the measurement setup [26]. We have tested several options. Aqueous REs, claimed to be leakage free, increased always systematically the water content of the electrolytes over time. Quasi REs haven't been stable over the duration of the experiments in the flow cell. A homemade RE consisting of a 1/16″ PEEK tube with a leakage-free frit and silver wire immersed in a methanol solution containing tetrabutylammonium perchlorate (0.1 mol L^{-1}) and $AgNO_3$ (0.01 mol L^{-1}) has been proven to be the

most appropriate RE for the measurements. According to the recommendations of IUPAC to report electrode potentials in nonaqueous electrolytes [27] the homemade RE was calibrated against the ferrocene/ferrocenium (Fc/Fc^+) redox couple and all potentials were referenced to E vs. Fc/Fc^+ (see Supporting Information for further information).

3.2. ICP-MS settings for organic samples

ICP-MS is a versatile method for the quantification of trace elements in different fields of science and industry. However, analysis are mostly performed in aqueous media [28].

The application of ICP-MS for organic solvents requires major adjustments at the instrument. First of all, the higher vapor pressure of many organic solvents compared to water causes a higher sample uptake rate into the plasma, leading to unstable plasma performance. A PC 3 Peltier cooler (PerkinElmer) was used to optimize the temperature of the spray chamber and reduce the sample amount introduced into the plasma. In order to reduce the sample uptake further, the diameter for all components of the sample introduction system were reduced. The high carbon content represents one of the central problems with organic samples causing soot deposition on the cones, leading to a variation of the opening of the cones which results in unstable signals or even cone blockage. This problem is overcome by adding small amounts of oxygen (5–10%) to the argon carrier gas. The amount of oxygen added has to be sufficient to prevent soot deposition but has to be limited, in order to sustain good sensitivity. The addition of oxygen to the carrier gas leads to more aggressive plasma operation conditions and the traditionally used Ni cones have to be replaced by more stable Pt cones. For every organic solvent the operation parameters have to be optimized individually [29]. The optimized ICP-MS settings for the measurements as well as information on the calibration of the instrument can be found in SI.

3.3. Dissolution behavior of Pt in 0.05 mol L^{-1} $LiClO_4$ containing MeOH

3.3.1. The effect of increased upper potential limit on Pt dissolution

The dissolution behavior of Pt in aqueous media has been extensively studied and there are well established explanations to the underlying mechanisms [7,19]. Two different potential dependent mechanisms govern the dissolution of Pt in aqueous media. These are the anodic dissolution, starting around 0.8 V vs. RHE, and the cathodic dissolution, characteristic to the Pt-O reduction region. During the anodic dissolution Pt is directly oxidized to form Pt^{2+} ions, whereas the mechanism of the cathodic dissolution is somewhat more complex: it requires the oxidation of the Pt surface first and appears during the negatively going scan simultaneously with the reduction of the surface oxide. The oxidation number and form of the dissolved species are still disputed [30]. In order to study the potential dependence of Pt dissolution in organic media, first cyclic voltammograms between –0.5 V and a changing upper potential limit (UPL) with a scan rate of 10 mV s^{-1} were measured. It is clear from ICP-MS data shown in Fig. 2a that independently of the UPL there is only one peak visible during the potential cycling, which corresponds to an anodic dissolution. The peak maxima of the dissolution profile are well aligned with the peak maxima of the potential curves. There is no peak observed indicating cathodic dissolution in this methanol-based electrolyte. The observation suggests that during the decomposition of MeOH (see Figs. S6, S8) there is no Pt-O formation which could induce passivation of the surface and hinder the dissolution during the anodic scan. This theory is supported by Fig. 2b showing the total dissolved amounts (TDA) of Pt per cycle. The TDA were calculated by integrating the Pt dissolution peaks and multiplying the results of the integration by the flow rate of the electrolyte (150 μL min^{-1}). The dependence of the TDA per cycle on the upper potential limit can be fitted with an exponential growth suggesting that a simple charge transfer reaction governs Pt dissolution. Since the rate of the main electrode reaction, i.e., methanol oxidation can also be described by an exponential curve, their ratio increases linearly over the different potential limits (see Fig. 2c). Assuming a two electron process, the Pt dissolution accounts to ca. 10^{-4}% of the total charge transferred during the anodic reactions. This observation contrasts the dissolution behavior in aqueous media where the anodic dissolution of Pt reaches a maximum upon the formation of an oxide layer. Even though the overall dissolution process is completely different, compared to aqueous solutions, an off-line analysis of samples taken at the end of each cycle could not reveal the real difference in the dissolution mechanism of Pt in the two systems. This can only be observed by on-line analysis. The amount of dissolved Pt, however, is similar to that observed in aqueous acidic solutions [15].

3.3.2. The effect of scan rate on Pt dissolution

It has been shown that the scan rate has a significant impact on the dissolution of Pt [15]. To be able to see this effect in methanol-based electrolyte cyclic voltammograms with scan rates of 2 mV s^{-1}, 5 mV s^{-1}, 10 mV s^{-1}, and 20 mV s^{-1} were recorded between −0.5 V and 0.9 V (see SI). Two CVs were measured at each scan rate and the second cycle of each measurement was used to calculate the TDA of Pt during the CVs. The TDA vs. scan rate curve shown in Fig. 3 exhibits an exponential decay with increasing scan rate, from 5.1 ng cm^{-2} $cycle^{-1}$ to 0.3 ng cm^{-2} $cycle^{-1}$ (for fitting parameters see SI). Similar findings have been reported for the scan rate dependence in aqueous media [15]. However, if the TDA is normalized by time (see Fig. 3 inset), a very similar trend can be observed, which is opposite to the results obtained in aqueous electrolytes. In methanol-based electrolyte the TDA per second monotonically declines with increasing scan rate, even though the amounts are very similar for 2 mV s^{-1} and 20 mV s^{-1} (3.8 pg cm^{-2} s^{-1} and 2.2 pg cm^{-2} s^{-1}, respectively). The opposite dissolution behavior can be explained by the absence of cathodic dissolution and the fact that the extent of anodic dissolution increases with the duration of anodic polarization, i.e. with decreasing scan rates. In aqueous media, however, at lower scan rates the potential is kept in the oxide formation region longer causing less anodic but more cathodic dissolution. Whereas during fast cycling less Pt-O is formed, therefore the anodic dissolution is faster and the cathodic dissolution is limited by the lower amount of the formed oxide.

3.3.3. The effect of CA duration on Pt dissolution

In organic electrosynthesis Pt is a widely applied electrode material due to its stability and inertness. The experiments are most commonly conducted at constant current or constant potential. An experiment was performed to investigate the stability of Pt under such conditions. Therefore, the potential of the working electrode was kept constant for different times at 700 mV, 800 mV and 900 mV (see SI). The TDA was calculated as well as the charge consumed when Pt is dissolved, using Faraday's law and assuming a two electron process. All step potential experiments show a monotonic increase with the duration of the potential step (see Fig. 4) reaching the highest dissolved amount at 900 mV applied for 120 s with 5.1 ng cm^{-2}. This corresponds to 1.2% of a monolayer of Pt, assuming the surface concentration of Pt atoms to be 1.37×10^{15} cm^{-2}. By the extrapolation of the fitted linear and assuming a 10 cm^2 big electrode 1.5 μg of platinum loss on the working electrode is to be expected during a 1 h chronoamperometric measurement. Another interesting observation is the increasing slope of TDA with step duration (t_d) from 700 mV to 900 mV, which is important to keep in mind when performing a reaction at constant potential. The mass loss of the electrode is rather negligible (in case of the 10 cm^2 electrode with a thickness of 50 μm, it is 0.007% per hour). However, the dissolved metal ions may catalyze homogeneous reactions in the bulk phase, contaminate the product of synthesis or by deposition on the counter electrode influence the counter reactions.

The charge, accounted for the dissolution of Pt is ca. 10^{-4}% of the total charge passed through the electrodes and increases with

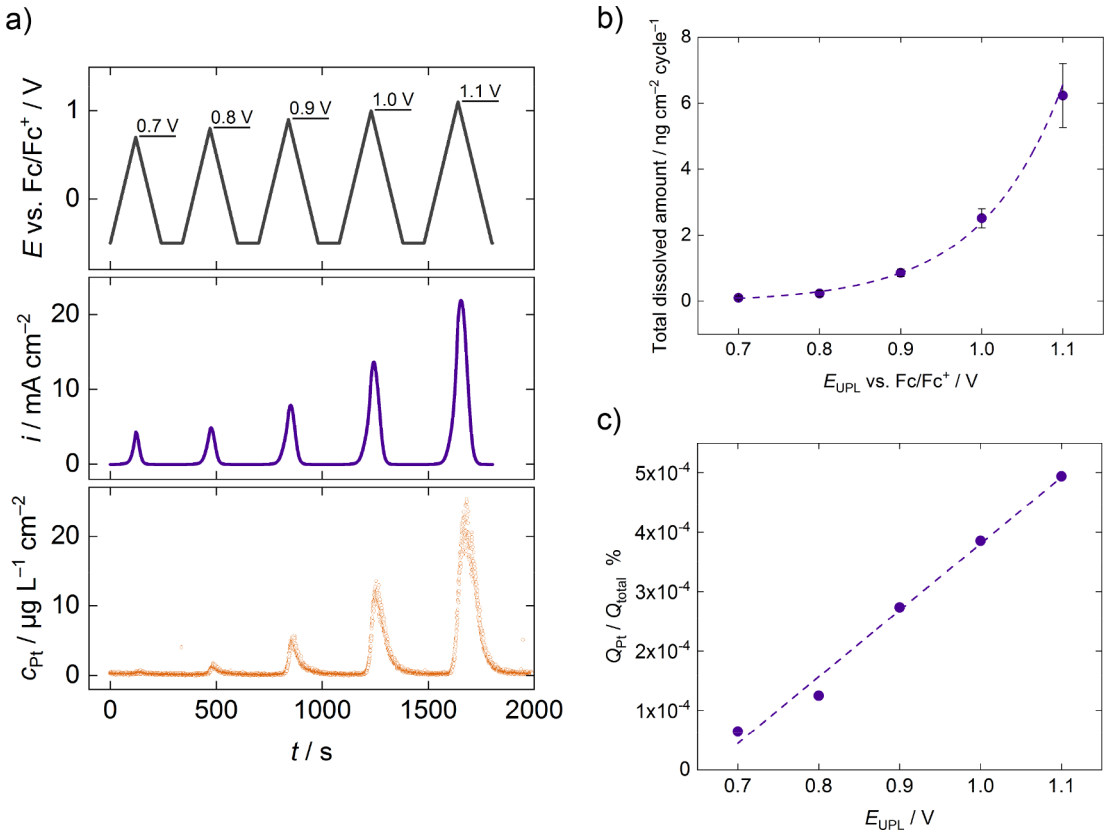

Fig. 2. a) Potential profile and corresponding current density vs. time and dissolved Pt concentration vs. time curves (for cyclic voltammograms see Fig. S6 in SI). The potential was cycled between −0.5 V and varying upper potential limits in the range of 0.7 V–1.1 V in 100 mV steps with a scan rate of 10 mV s^{-1} in 0.05 mol L^{-1} $LiClO_4$ containing MeOH solution. b) Calculated total dissolved amount of Pt per cycle with different upper potential limits. c) Calculated Pt dissolution charge ratio.

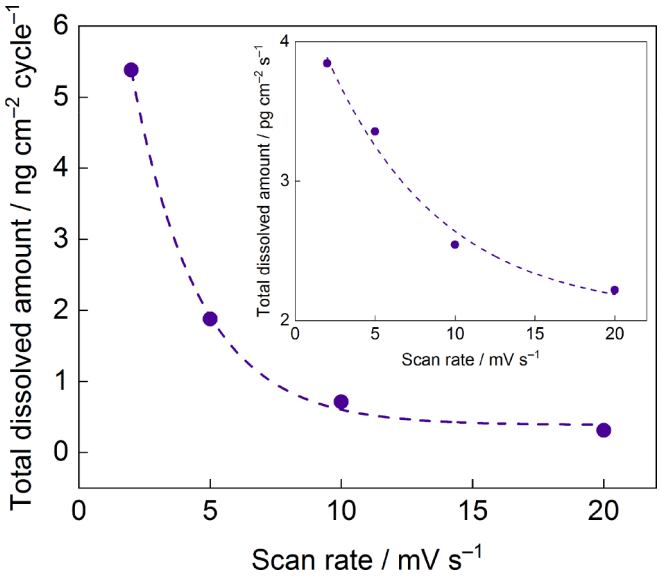

Fig. 3. Calculated amounts of dissolved Pt in 0.05 M $LiClO_4$ containing MeOH solution during cyclic voltammetry with scan rates of 2 mV s^{-1}, 5 mV s^{-1}, 10 mV s^{-1}, 20 mV s^{-1} per cycle and per second (inset).

increasing potential. The charge fraction of Pt dissolution is almost constant at 700 mV independent of the step duration and slightly decreases at higher potentials with the step duration. This could be due to the residual water in the solution (ca. 37 ppm) slowly diffusing to the surface of the working electrode, reacting with Pt and forming Pt-O species, which hinder anodic dissolution. This amount is, however, so small, that cathodic dissolution is not detectable. The influence of water impurities on the dissolution of Pt goes beyond this manuscript and is the subject of future studies.

4. Conclusion

In this work we primarily showed the development and capabilities of an EFC operated in a glovebox and coupled to an ICP-MS for non-aqueous electrolytes on the example of Pt metal. We demonstrated that – contrary to aqueous electrolytes – in $LiClO_4$ containing methanol-based electrolyte Pt only exhibits one type of dissolution, which is the anodic one. During a scan rate study, it was revealed that the amount of dissolved Pt increases exponentially with decreasing scan rate, regardless whether the dissolved amount is normalized to cycles or time. Furthermore, we pointed out, that due to the lack of formation of a protecting oxide layer, Pt is constantly dissolving at high enough anodic potentials; a typical case during experiments in electroorganic synthesis. The influence of trace amounts of water and other impurities on the dissolution of platinum will be subject of following studies. This novel method can be applied in the future to study the stability of different systems, like nonaqueous batteries or catalysts used in the electroorganic synthesis.

CRediT authorship contribution statement

Johanna Ranninger: Conceptualization, Methodology, Investigation, Writing - original draft, Visualization. **Susanne J. Wachs:** Methodology. **Jonas Möller:** Software. **Karl J.J. Mayrhofer:** Writing - review & editing, Funding acquisition. **Balázs B. Berkes:** Conceptualization, Methodology, Software, Writing - review & editing, Supervision.

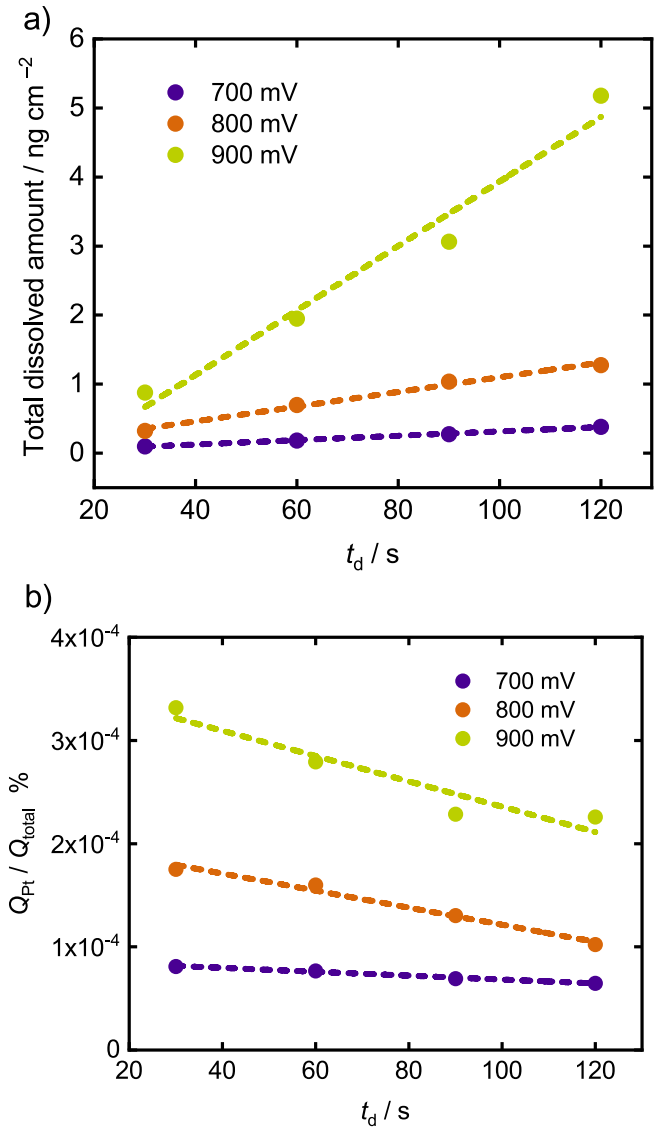

Fig. 4. a) Calculated total dissolved amount of Pt and b) charge ratios corresponding to dissolution during the potential step measurements at potentials 700 mV (purple circles), 800 mV (orange circles) and 900 mV (green circles) for 30, 60, 90 and 120 s. (For interpretation of the references to colour in this figure legend, the reader is referred to the web version of this article.)

Acknowledgement

This work was supported by the German Research Foundation (DFG) under Germany's Excellence Strategy – Exzellenzcluster 2186 "The Fuel Science Center".

Appendix A. Supplementary data

Supplementary data to this article can be found online at https://doi.org/10.1016/j.elecom.2020.106702.

References

[1] P.G. Bruce, S.A. Freunberger, L.J. Hardwick, J.M. Tarascon, Nat. Mater. 11 (2011) 19–29.
[2] N.S. Choi, Z. Chen, S.A. Freunberger, X. Ji, Y.K. Sun, K. Amine, G. Yushin, L.F. Nazar, J. Cho, P.G. Bruce, Angew. Chem. Int. Ed. 51 (2012) 9994–10024.
[3] X. Han, K. Wang, G. Zhang, W. Gao, J. Chen, Adv. Synth. Catal. 361 (2019) 2804–2824.
[4] S. Mohle, M. Zirbes, E. Rodrigo, T. Gieshoff, A. Wiebe, S.R. Waldvogel, Angew. Chem. Int. Ed. 57 (2018) 6018–6041.
[5] J.P. Grote, A.R. Zeradjanin, S. Cherevko, K.J. Mayrhofer, Rev. Sci. Instrum. 85 (2014) 104101.
[6] B.B. Berkes, A. Jozwiuk, M. Vracar, H. Sommer, T. Brezesinski, J. Janek, J. Anal. Chem. 87 (2015) 5878–5883.
[7] S. Cherevko, A.R. Zeradjanin, A.A. Topalov, N. Kulyk, I. Katsounaros, K.J.J. Mayrhofer, ChemCatChem 6 (2014) 2219–2223.
[8] P. Jovanovič, A. Pavlišič, V.S. Šelih, M. Šala, N. Hodnik, M. Bele, S. Hočevar, M. Gaberšček, ChemCatChem 6 (2014) 449–453.
[9] J. Knöppel, S. Zhang, F.D. Speck, K.J.J. Mayrhofer, C. Scheu, S. Cherevko, Electrochem. Commun. 96 (2018) 53–56.
[10] P.P. Lopes, D. Strmcnik, D. Tripkovic, J.G. Connell, V. Stamenkovic, N.M. Markovic, ACS Catal. 6 (2016) 2536–2544.
[11] S.O. Klemm, A.A. Topalov, C.A. Laska, K.J.J. Mayrhofer, Electrochem. Commun. 13 (2011) 1533–1535.
[12] A.K. Schuppert, A.A. Topalov, I. Katsounaros, S.O. Klemm, K.J.J. Mayrhofer, J. Electrochem. Soc. 159 (2012) F670–F675.
[13] S. Cherevko, S. Geiger, O. Kasian, N. Kulyk, J.-P. Grote, A. Savan, B.R. Shrestha, S. Merzlikin, B. Breitbach, A. Ludwig, K.J.J. Mayrhofer, Catal. Today 262 (2016) 170–180.
[14] S. Geiger, O. Kasian, M. Ledendecker, E. Pizzutilo, A.M. Mingers, W.T. Fu, O. Diaz-Morales, Z. Li, T. Oellers, L. Fruchter, A. Ludwig, K.J.J. Mayrhofer, M.T.M. Koper, S. Cherevko, Nat. Catal. 1 (2018) 508–515.
[15] A.A. Topalov, I. Katsounaros, M. Auinger, S. Cherevko, J.C. Meier, S.O. Klemm, K.J. Mayrhofer, Angew. Chem. Int. Ed. 51 (2012) 12613–12615.
[16] P. Jovanovič, V.S. Šelih, M. Šala, N. Hodnik, N.P.J. Mater, Degrad. 2 (2018) 9.
[17] P.P. Lopes, M. Zorko, K.L. Hawthorne, J.G. Connell, B.J. Ingram, D. Strmcnik, V.R. Stamenkovic, N.M. Markovic, J. Phys. Chem. Lett. 9 (2018) 4935–4940.
[18] J. Wandt, A. Freiberg, R. Thomas, Y. Gorlin, A. Siebel, R. Jung, H.A. Gasteiger, M. Tromp, J. Mater. Chem. A 4 (2016) 18300–18305.
[19] G. Inzelt, B. Berkes, Á. Kriston, Electrochim. Acta 55 (2010) 4742–4749.
[20] G. Inzelt, B.B. Berkes, Á. Kriston, Pure Appl. Chem. 83 (2010) 269–279.
[21] A.A. Topalov, S. Cherevko, A.R. Zeradjanin, J.C. Meier, I. Katsounaros, K.J.J. Mayrhofer, Chem. Sci. 5 (2014) 631–638.
[22] N. Kulyk, S. Cherevko, M. Auinger, C. Laska, K.J.J. Mayrhofer, J. Electrochem. Soc. 162 (2015) H860–H866.
[23] D. Aurbach, I. Weissman, Nonaqueous Electrochemistry, Marcel Dekker Inc, New York, 1999, pp. 30–38.
[24] R. Thomas, Practical Guide to ICP-MS, Marcel Dekker Inc., New York, 2004.
[25] Q. Zhang, J.T. Snow, P. Holdship, D. Price, P. Watson, R.E.M. Rickaby, J. Anal. At. Spectrom. 33 (2018) 1196–1208.
[26] D. Aurbach, A. Zaban, Nonaqueous Electrochemistry, Marcel Dekker Inc, New York, 1999, pp. 104–106.
[27] J.K.G. Gritzner, Pure Appl. Chem. 56 (1984) 461–466.
[28] A.A. Ammann, J. Mass Spectrom. 42 (2007) 419–427.
[29] R.C. Hutton, J. Anal. At. Spectrom. 1 (1986) 259–263.
[30] Y. Sugawara, T. Okayasu, A.P. Yadav, A. Nishikata, T. Tsuru, J. Electrochem. Soc. 159 (2012) F779–F786.